JOURNAL OF MATERIALS SCIENCE 27 (1992) 203–209

Welding of thin steel plates: a new model for thermal analysis

B. V. KUMAR, O. N. MOHANTY
National Metallurgical Laboratory, Jamshedpur 831 007, India
A. BISWAS
Metallurgical Engineering, Indian Institute of Technology, Kharagpur 721 302, India

A mathematical model for the transient heat flow analysis in arc-welding processes is proposed, based on a unique set of boundary conditions. The model attempts to make use of the relative advantages of analytical as well as numerical techniques in order to reduce the problem size for providing a quicker solution without sacrificing the accuracy of prediction. The variation of thermo-physical properties with temperature has been incorporated into the model to improve the thermal analysis in the weld and heat-affected zones. The model has been evaluated using a five-point explicit finite difference method for analysing the welding heat flow in thin plates of two different geometric configurations. The temperature distribution closer to the heat source, primarily in the weld zone and the heat-affected zones, are predicted by the numerical technique. The thermal characteristics beyond the heat-affected zone are amenable to standard analytical techniques. The behaviour of the boundary condition in the model has been investigated in detail.

1. Nomenclature

q'	Rate of heat per unit thickness ($W\,m^{-1}$)
d	Plate thickness (m)
v	Velocity of source ($m\,s^{-1}$)
t	Time (s)
T	Temperature value at the desired point (K)
T_0	Initial temperature (K)
k	Thermal conductivity ($W\,m^{-1}\,K^{-1}$)
ρ	Density ($kg\,m^{-3}$)
c_p	Specific heat ($J\,kg^{-1}\,K^{-1}$)
α	Thermal diffusivity ($m^2\,s^{-1}$)
n	$\dfrac{q'v}{4\pi\alpha^2\rho c_p(T_{A_{e3}} - T_0)}$ (m^{-1})
ξ	Distance of point considered from the source ($\xi = x - vt$) (m)
K_0	Modified Bessel function of second kind and zero order
r	Radial distance from the source ($r = (x^2 + y^2)^{1/2}$) (m)
ω	Model width (m)
a	Plate width (m)
ε	Distance from the source $\varepsilon = (\xi^2 + 4 \times 10^{-4})^{1/2}$ (m)
μ_n	$\left[1 + \left(\dfrac{\pi n 2\alpha}{va} - \right)\right]^{1/2}$

2. Introduction

The transient temperature field produced by a moving heat source, such as an arc, has profound influence on the properties of the material close to the heat source, and the material is modified in structure as well as in properties due to a variety of phase transformations. The analysis of welding heat flow, thus assumes importance as the basis for the understanding of physio-mechanical properties of welded structures. Initial attempts at heat flow analysis were analytical in nature [1]. Rosenthal [2, 3] is credited with developing the first analytical solution for heat flow analysis in one, two and three dimensions. The application of analytical solutions to the real situation indicated an excellent correlation away from the heat source [1–3]. This region can be identified as that portion of the material undergoing only Newtonian heating and cooling cycles. Appreciable departures from the real situation were, however, observed close to the heat source. The limitation of the analytical solution in the close proximity of the heat source may be attributed to the simplifying assumptions (such as point/linear source, temperature-independent properties, etc.) made while deriving the analytical solutions. Attempts [4, 5] to incorporate more realistic terms in Rosenthal's solution could only provide limited success in the vicinity of the heat source. However, the use of numerical methods coupled with powerful digital computers, have allowed more detailed analysis of the heat flow in this region. The advantage of the proposed numerical technique lies in its ability to handle complex geometries, variation of material properties with temperature, phase transformations, etc. These numerical techniques, such as the finite difference method (FDM) and finite element method (FEM), yield better temperature predictions close to the heat

0022–2461/92 $03.00 + .12

source, and can also compute residual stress and microstructure, etc., which are helpful in rationalizing the ultimate physio-mechanical behaviour of weldments [6–10]. These methods, traditionally consider discretization of the entire system, and therefore can be time-consuming and expensive.

The present investigation examines the possibility of developing a combined model using the advantages of analytical as well as numerical methods, thus cutting down on expensive computation time, whilst maintaining accuracy; such attempts do not appear to have been made earlier, although similar views have been expressed in the literature [11]. The present paper is part of a comprehensive programme [12], that includes forecasting the size of the heat-affected zone (HAZ) and microstructure, etc., using the thermal behaviour predicted from the model.

3. Mathematical model

The model has been formulated for two distinct geometric configurations. The first, termed the infinite case, deals with a situation wherein welding heat flow in large, thin plates is simulated. A similar treatment for plates of finite width, termed the semi-infinite case, is then carried out.

3.1. Physical model

The case discussed here relates to butt-welding two flat plates between which an intense heat source, such as an arc, moves with a constant velocity. The energy input per unit thickness of the plate was assumed to be constant. The path of the source coincided with the axis of symmetry of the system. The regions of the plates close to the moving heat source melt and thus welding proceeds. The illustration in Fig. 1a depicts the infinite situation. The plates are assumed to extend to infinity in the x- and y-directions, and, hence, can be designated an infinite system [13, 14]. Fig. 1b illustrates the case where the plate width (measured along the y-direction) is finite, while the plate length (measured along the x-direction and the direction of welding) extends to infinity.

3.2. Assumptions

The model has been formulated using the following assumptions.

1. The mode of heat transfer in the plates is strictly conductive and restricted to the x–y plane only.
2. Convective heat transfer within the weld pool is simulated by the use of thermal properties of the liquid metal such as thermal conductivity, specific heat and density.
3. Heat losses through vaporization of the material in the fusion zone are neglected.
4. Convection and radiation losses perpendicular to the plane of the plate are neglected.
5. Heat flow is symmetrical with respect to the geometric axis of symmetry.
6. Material properties such as thermal conductivity, specific heat and density, etc., have a definite functional relationship with temperature.
7. The size of the heat source is equal to that of the element in the model adjacent to the axis of symmetry.

3.3. Problem formulation and boundary conditions

The basic equation of heat conduction in two dimensions in a solid is

$$\frac{\partial}{\partial x}\left(k\frac{\partial T}{\partial x}\right)+\frac{\partial}{\partial y}\left(k\frac{\partial T}{\partial y}\right)+Q = \rho c_p\frac{\partial T}{\partial t} \quad (1)$$

where k, ρ and c_p denote the thermal conductivity, density and specific heat of the material, and Q is the heat generation term. The variation of these thermophysical properties of steel with temperature is expressed as follows [15]:

$$\left.\begin{aligned} k &= 75.00 - 0.073\,T + 0.205\times10^{-4}\,T^2 \ \mathrm{W\,m^{-1}\,K^{-1}} \quad (2)\\ c_p &= 416.0 + 0.637\,T - 0.252\times10^{-3}\,T^2 \ \mathrm{J\,kg^{-1}\,K^{-1}} \quad (3)\\ \rho &= 7950 - 0.162\,T - 0.175\times10^{-3}\,T^2 \ \mathrm{kg\,m^{-3}} \quad (4)\end{aligned}\right\} \forall\ T,\quad 27 \le T \le T_m$$

The mathematical analysis of heat flow in a weldment for the present case is essentially a solution of Equation 1 for a set of given initial and boundary conditions.

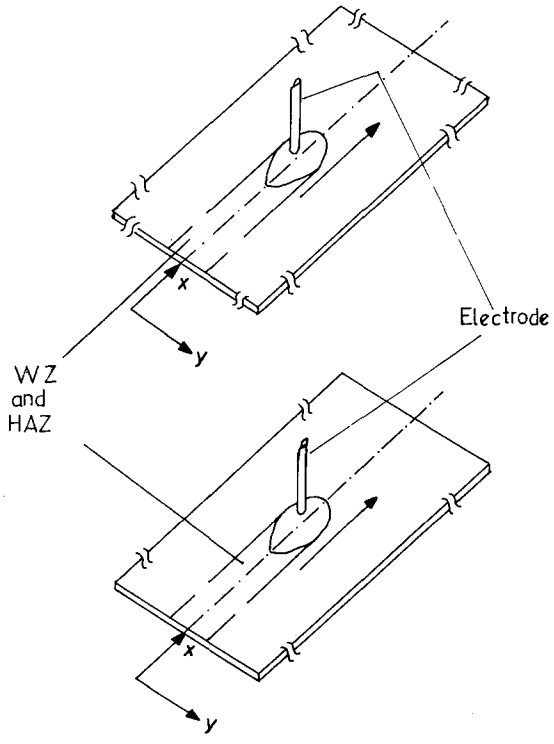

Figure 1 Physical model of butt-welding of thin plates representing (a) an infinite case and (b) a semi-infinite case.

3.3.1. Initial condition

The initial temperature distribution in the material being welded defines the initial condition. Assuming that there is no preheating, the initial condition may be mathematically stated as follows:

$$\text{At} \quad t = 0, \; T(x, y) = T_0 \; \forall \; x, y \tag{5}$$

3.3.2. Boundary conditions

An axi-symmetric boundary condition, also termed the Neumann condition [16], is imposed along the welding central line depicted in Fig. 1. Accordingly

$$\left.\begin{array}{l}\text{At} \quad y = 0 \\ \text{and} \quad t > 0\end{array}\right\} -k\frac{\partial T}{\partial y} = 0 \; \forall \; x \tag{6}$$

3.3.2.1. Infinite case.

$$\left.\begin{array}{l}\text{At} \quad x = 0 \\ \quad\; x = 1 \\ \text{and} \quad t > 0\end{array}\right\} T = T_0 + \frac{q'}{2\pi k} e^{-(v\xi/2\alpha)} K_0\left(\frac{vr}{2\alpha}\right) \forall \; y \tag{7a}$$

or

$$T = T_0 + \frac{q'}{2\pi k} e^{-(v/2\alpha)(\xi + r)} \left(\frac{\pi\alpha}{vr}\right)^{1/2} \forall \; y \tag{7b}$$

$$\left.\begin{array}{l}\text{At } y = a \\ \text{and } t > 0\end{array}\right\} T = T_0 + \frac{q'}{2\pi k} e^{-(v\xi/2\alpha)} K_0\left(\frac{v\varepsilon}{2\alpha}\right) \forall \; x \tag{8a}$$

or

$$T = T_0 + \frac{q'}{2\pi k} e^{-(v/2\alpha)(\xi + \varepsilon)} \left(\frac{\pi\alpha}{v\varepsilon}\right)^{1/2} \forall \; x \tag{8b}$$

The narrow portion of the plate chosen between the boundary limits $y = 0$ to $y = a$ forms the width a of the model. This width is a function of welding speed and the energy input, and can be calculated with the help of an equation suggested by Adams [17] by substituting $0.3\,T^m$ in place of the peak temperature. However, an optimized width of 0.02 m was chosen throughout the present investigation. It is now evident from the boundaries of the hypothetical plate defined above, that the model area would be a very small fraction of the total area of the plate.

3.3.2.2. Semi-infinite case.

$$\left.\begin{array}{l}\text{At} \quad x = 0 \\ \quad\; x = 1 \\ \text{and} \quad t > 0\end{array}\right\} T = T_0 + \frac{q'}{\pi k} e^{-(v\xi/2\alpha)} \sum_{n=-\infty}^{n=\infty} K_0\left(\frac{r_n v}{2\alpha}\right) \forall \; y \tag{9}$$

$$\left.\begin{array}{l}\text{At} \quad y = a \\ \text{and} \quad t > 0\end{array}\right\} T = T_0 + \frac{q'}{\pi k} e^{-(v\xi/2\alpha)} \sum_{n=-\infty}^{n=\infty} K_0\left(\frac{r_n v}{2\alpha}\right) \forall \; x \tag{10}$$

A simplified version of this boundary condition can be obtained by transforming Equation 9 or 10 into a Fourier series [3]. Accordingly, Equations 11a and b, as shown below, can be used in place of Equation 9, depending on the value of ξ.

$$\left.\begin{array}{l}\text{At} \quad x = 0 \\ \quad\; x = 1 \\ \text{and} \quad t > 0\end{array}\right\} T = T_0 + \frac{q'}{c_p \rho \omega v}\left[e^{-(v\xi/\alpha)} + \sum_{n=1}^{n=\infty} \frac{2}{\mu_n} e^{-[(\mu_n + 1)v\xi]/2\alpha} \cos\left(\frac{n\pi y}{\omega}\right)\right] \forall \; y \tag{11a}$$

for $\xi > 0$, and

$$T = T_0 + \frac{q'}{c_p \rho \omega v} \times \left[1 + \sum_{n=1}^{n=\infty} \frac{2}{\mu_n} e^{[(\mu_n - 1)v\xi]/2\alpha} \cos\left(\frac{n\pi y}{\omega}\right)\right] \forall \; y \tag{11b}$$

for $\xi < 0$.

Similarly, Equations 12a and b, as given below, may be used for evaluating the boundary condition given in Equation 10.

$$\left.\begin{array}{l}\text{At} \quad y = a \\ \text{and} \quad t > 0\end{array}\right\} T = T_0 + \frac{q'}{c_p \rho \omega v}\left[e^{-(v\xi/\alpha)} + \sum_{n=1}^{n=\infty} \frac{2}{\mu_n} e^{-[(\mu_n + 1)v\xi]2\alpha} \cos\left(\frac{n\pi\varepsilon}{\omega}\right)\right] \tag{12a}$$

for $\xi > 0$, and

$$T = T_0 + \frac{q'}{c_p \rho \omega v}\left[1 + \sum_{n=1}^{n=\infty} \frac{2}{\mu_n} e^{[(\mu_n - 1)v\xi]/2\alpha} \cos\left(\frac{n\pi\varepsilon}{\omega}\right)\right] \tag{12b}$$

for $\xi < 0$.

The geometrical width of the model, between the limits $y = 0$ to $y = a$, corresponds to a as indicated in the previous case. A comparison between Equation 12 and Equation 8 would indicate that the temperature value in the y-direction in the semi-infinite case is influenced by the finite width, ω, of the plate.

The model, thus defined by the initial condition (Equation 5) along with boundary conditions as described previously (Equations 6–8 for the infinite case and Equations 6, 9–12 for the semi infinite case) can be appropriately termed the mixed boundary model (MBM).

3.4. Solution procedure

A five-point explicit finite difference technique was chosen for the evaluation of both cases. The system was discretized into a fine mesh. The grid-spacing in the x-direction was kept constant at 3.33×10^{-3} m. A variable grid-spacing was employed in the y-direction. The grid spacing close to the heat source was 8.33×10^{-4} m, while the spacing in the rest of the plate was 3.33×10^{-3} m. The time-stepping in the algorithm is based on a check on the stability criteria [18].

4. Results and observations

4.1. Infinite case

The development of various transient temperature fields in an infinite plate, in the narrow strip as defined

by the boundaries of Equations 6–8, at two different time intervals, are presented in Figs 2 and 3 in the form of dimensionless maps. The dimensionless isotherms on this map, as well as on the others, are also based on the reference temperature, A_{e3}, of steel. These maps are generated by using dimensionless groups from the literature [19]. Such groups used in this context are listed in Table I. The figures illustrate isotherms for a hypothetical welding situation of steel plates. An operating parameter of 0.25 was used in computing these maps.

The isotherms drawn in Fig. 4 are the superimposition of contours for different values of operating parameters at a constant value of dimensionless time. A similar presentation in Fig. 5 is made, where the contours are superimposed for a case in which both operating parameter and dimensionless time are varied. The dimensionless distance in the welding direction, as well as in the transverse direction, depicted in Fig. 5, are based on an average velocity of $3.5 \times 10^{-3}\ \mathrm{m\,s^{-1}}$.

TABLE I Dimensionless groups

Symbol	Name	Description
η	Operating parameter	$\dfrac{qv}{4\pi\alpha^2\rho c_p(T_{A_{e3}} - T_0)}$
θ	Dimensionless temperature	$\dfrac{T - T_0}{T_{A_{e3}} - T_0}$
ζ	Dimensionless x-axis	$\dfrac{vx}{2\alpha}$
ψ	Dimensionless y-axis	$\dfrac{vx}{2\alpha}$
∂	Effective thickness	$\dfrac{vd}{2\alpha}$
τ	Dimensionless time	$\dfrac{v^2 t}{2\alpha}$

4.2. Semi-infinite case

The dimensionless maps of isotherms, for the semi-infinite case, are given in Figs 6–8. Fig. 6 represents a typical pattern of temperature distribution due to the moving heat source satisfying the boundary conditions defined in Equations 6, 9 and 10. Figs 7 and 8 are diagrams in which the isotherms for different values of operating parameters are superimposed for comparison. Fig. 7 compares the variation in the isotherms due to the variation in the operating parameter. The isotherms are obtained at $\tau = 12.95$. A similar superimposition of isotherms for various values of operating parameters is made in Fig. 8. Here, the dimensionless distance along the welding direction,

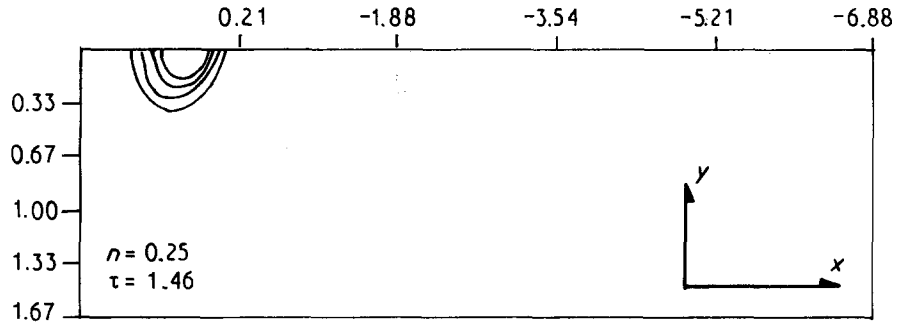

Figure 2 Dimensionless map depicting isotherms in the hypothetical plate at $\tau = 1.46$. The values of the isotherms plotted are 0.24, 0.38, 0.54 and 0.67.

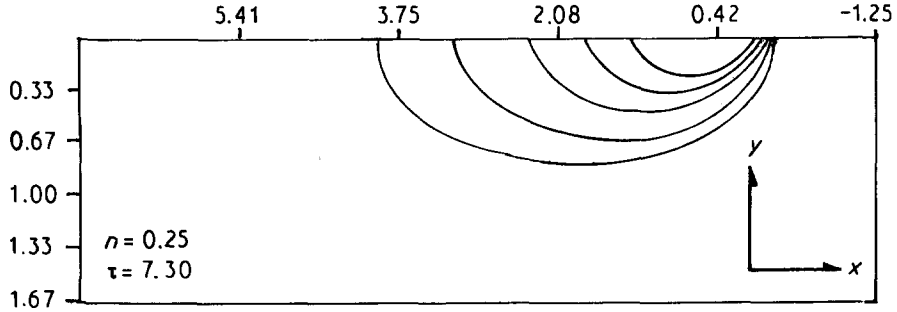

Figure 3 Dimensionless map depicting isotherms in the hypothetical plate at $\tau = 7.3$. The values of the isotherms plotted are 0.24, 0.38, 0.54, 0.67 and 0.81.

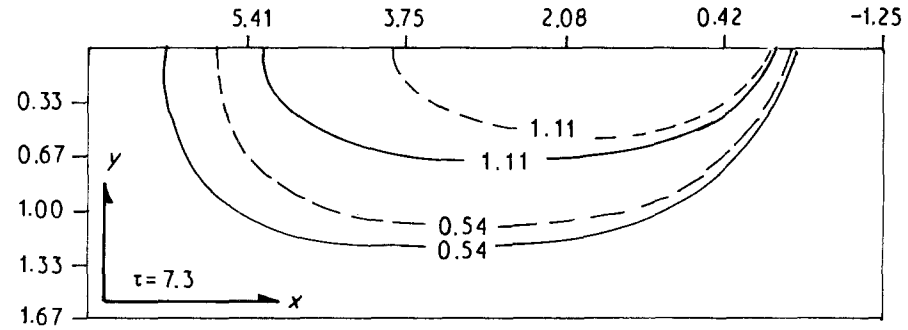

Figure 4 Variation of temperature distribution with respect to operating parameter. Dimensionless temperatures of 1.11 and 0.54 are compared. (---) $n = 0.40$, (——) $n = 0.53$.

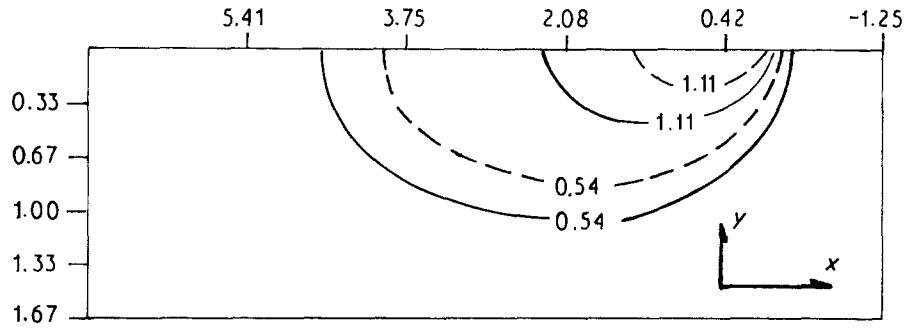

Figure 5 Comparison of dimensionless isotherms at $v = 3.5 \times 10^{-3}\ \mathrm{m\,s^{-1}}$. Operating parameter and dimensionless time are varied. (——), $n = 0.19$, $\tau = 5.2$; (---) $n = 0.25$, $\tau = 7.3$.

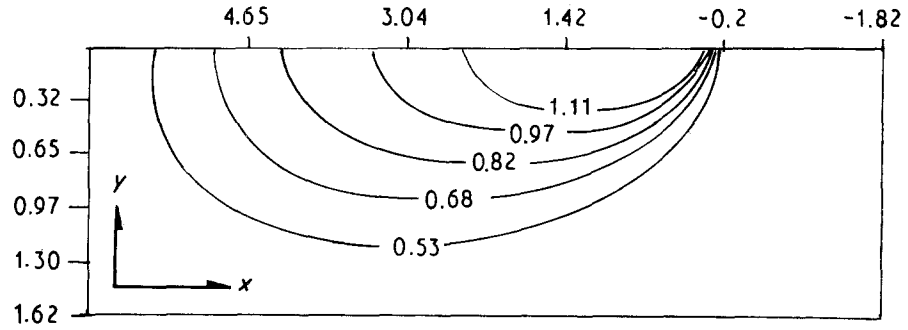

Figure 6 Dimensionless map depicting a typical temperature distribution in the hypothetical semi-infinite plate. The values of the isotherms are inscribed on the contours. $\tau = 6.48$, $n = 0.06$.

as well as in the transverse direction, is based on an average welding velocity of $5.4 \times 10^{-3}\ \mathrm{m\,s^{-1}}$.

5. Discussion

The temperature distribution predicted by the model in the hypothetical narrow strip is now based on a non-conventional set of variable boundary conditions. Hence, the behaviour of the model will be crucially dependent on the governing boundary conditions and the assumptions made while deriving the model. While some of the assumptions mentioned earlier are self explanatory, a few would warrant further elucidation.

The correlation of theoretical cooling rates at the top and the bottom of the plates on the welding central line is an indication of the dimension of heat flow (e.g. [20]). Accordingly, when the cooling rates on the central line at the top and the bottom of the plate being welded are identical for a plate of a particular relative thickness, the heat flow is said to be restricted to two dimensions. The heat flow along the thickness of the plate would be negligible. Depending on the welding operating parameter employed in this exercise, it has been proved [12, 20] that Assumption 1 is valid in the present context.

Assumptions 3 and 4 are basically simplifications. Assumption 3 can be considered valid in the present context as the specific welding energy input range employed results only in a narrow zone of melting and hence will not lead to appreciable material and heat loss through vaporization. Similar argument can be extended to validate Assumption 4, that the possible heat loss due to radiation from a narrow (under the present energy-input range) zone will not seriously affect the cooling rate. The non-accountability in radiation loss will result in an increase in peak temperature. However, any change in peak temperature has been found to have only a marginal effect on the cooling rate in the temperature range 1073–773 K, which is the crucial range as far as the present predictions are concerned.

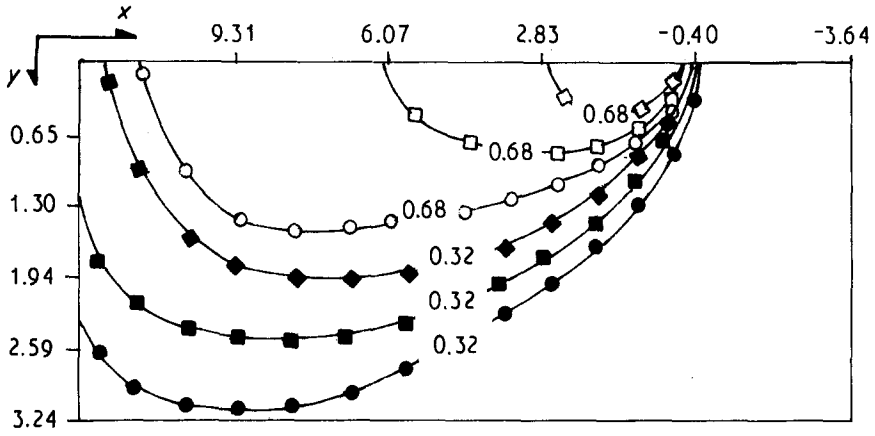

Figure 7 Superimposition of isotherms for different values of operating parameters. The inscribed numbers are the values of isotherms plotted. $\tau = 12.95$. n: (◆, ◇) 0.14, (■, □) 0.16, (●, ○) 0.19.

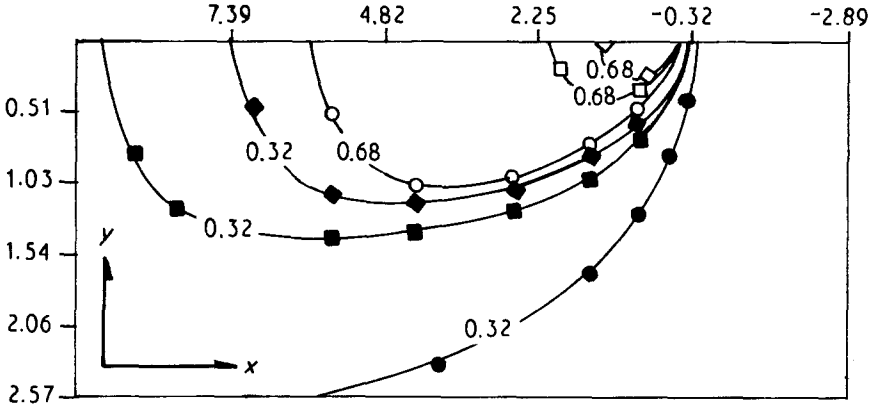

Figure 8 Comparison of dimensionless isotherms at $v = 5.4 \times 10^{-3}\ \mathrm{m\,s^{-1}}$. Operating parameter and dimensionless time are varied. The numbers inscribed on the contours are the values of isotherms. (◆, ◇) $n = 0.12$, $\tau = 12.95$; (■) $n = 0.10$, $\tau = 10.29$; (□) $n = 0.10$, $\tau = 12.27$; (●, ○) $n = 0.06$, $\tau = 6.48$.

A similar explanation would validate Assumption 7. If the source size (or shape), contrary to this assumption, is spread over multiple elements, the predicted peak temperatures will be only less than the actual value. However, as before, this would not affect the cooling rate in the range 1073–773 K, which is crucial for predicting the microstructure of the steel [21].

The transient temperature distribution at $\tau = 1.45$ (Fig. 2) and at $\tau = 7.30$ (Fig. 3) shows a gradual change in the temperature distribution pattern. The first observation is that the distribution predicted by the model, is in agreement with the expected behaviour in which the highest temperature domain is limited nearest to the heat source, with lower temperature zones fanning out. However, the distributions predicted at small times by this model presents a slightly different situation from reality. The temperature close to the "tail" portion of the contours drawn indicates a higher value than expected. This phenomenon may be termed a "pinched effect" and could be attributed to the boundary condition defined on the physical boundary line at $x = 0$, $\forall\ y$, particularly at small values of τ, by Equation 7 as elucidated below.

A detailed analysis of the boundary condition (Equation 7 for an infinite situation and Equations 6 or 11 for the semi-infinite situation) which is applicable at this physical boundary line, indicates that the thermal gradient in the welding direction, as one moves away from the source on either side, tends to zero [3, 22]. Mathematically

$$\lim_{\xi \to \pm\infty} \frac{\partial T}{\partial \xi} = 0 \tag{13}$$

and

$$\lim_{\xi \to \pm\infty} T = T_0 \tag{14}$$

However, using Equations 7–9 and 11

$$\lim_{\substack{\xi \to 0 \\ y \to 0}} T = \infty \tag{15}$$

Thus at small values of τ, the situation predicted by the boundary condition is close to Equation 15. Hence, the temperature predicted by these equations at this boundary would be quite large. Depending on the loci of the source, the temperature at the boundary may be, sometimes, greater than the source temperature itself according to Equation 13. A similar analysis of the boundary condition (Equation 8 in the infinite case and Equations 10 or 12 in the case of a semi-infinite system) also indicates that the thermal gradient approaches zero in the transverse direction [3]. Mathematically

$$\lim_{y \to \pm\infty} \frac{\partial T}{\partial y} = 0 \tag{16}$$

and

$$\lim_{y \to \pm \infty} T = T_0 \qquad (17)$$

The "pinched effect" thus deteriorates as one moves away from the source in the y-direction even at small values of τ. In fact, this effect vanishes more rapidly as the source moves away from the physical boundary line defined at $x = 0$, $\forall\ y$, and will not be effective on the physical boundary line defined by the limits $x = a$, $\forall\ y$.

The analysis of Equation 10 (or Equation 12) indicates that the thermal gradient in the transverse direction equals zero at the physical boundary of the semi-infinite solid. Mathematically

$$\frac{\partial T}{\partial y} \to 0 \quad \text{and} \quad T \to T_0 \text{ as } y \to a \qquad (18)$$

where once again a forms the geometrical width of the semi-infinite plate and ω is the width of the plate. It should be borne in mind that the quantity ω, the width of the strip, would be only a small fraction of the total width of the plate. Mathematically, $a \ll \omega$. Further details regarding these conditions and the choice of a are discussed elsewhere [12]. The difference in the temperature distribution in the lower temperature range, particularly in the transverse direction and away from the line of welding, may thus be attributed to the condition implied in Equation 18.

The semi-infinite case presents an additional problem at the boundary as predicted by Equations 11a and b. An inspection of these equations indicates that the solution involves the summation of the terms whose contribution to temperature becomes significant. At small values of τ the source location is closer to the boundary $x = 0$, $\forall\ y$, hence the number of terms for summation required to predict temperature accurately becomes exceedingly large. A compromise regarding the accuracy of temperature in order to circumvent this problem at this juncture cannot be made, as this could result in erratic behaviour of the solution.

Although it does not form a part of the present paper, it may be mentioned that temperature profiles for the chosen case have also been predicted by the authors elsewhere [12] using the more conventional FDM and FEM techniques and an excellent correlation has been observed. Thus, a high degree of confidence in the use of MBM is assured.

6. Conclusion

A novel approach, based on the combination of numerical and analytical methods, termed the mixed boundary model (MBM), has been attempted for predicting the transient thermal behaviour of the welded material close to the heat source in arc welding. Two different configurations, infinite and semi-infinite, have been studied. By shrinking the effective model area, the method appreciably reduces the extent of computational work without in any way affecting the accuracy.

References

1. P. S. MYERS, O. A. UYEHARA and G. L. BORMAN, *Weld. Res. Council Bull.* **123** (1967) 1.
2. D. ROSENTHAL, *Weld J.* **20** (1941) 220-s.
3. *Idem., Trans ASME* **68** (1946) 848.
4. R. J. GROSH, E. A. TRABANT and G. A. HAWKINS, *Q. Appl. Math.* **13** (1955) 61.
5. D. T. SWIFTHOOK and A. E. F. GICK, *Weld J.* **52** (1973) 492-s.
6. K. MASUBUCHI, "Analysis of Welded Structures" (Pergamon Press, 1980) p. 60.
7. S. KOU, T. KANEVSKY and S. FYFITCH, *Weld J.* **61** (1982) 175-s.
8. J. H. ARGYRIS, J. SZIMMAT and K. J. WILLIAM, "Numerical Methods in Heat Transfer" (Wiley, 1985).
9. P. TEKRIWAL, M. STITT and J. MAZUMDER, *Metal Constr.* **19** (1987) 559R.
10. T. ZACHARIA, S. A. DAVID, J. M. VITEK and T. DEBROY, *Metall Trans.* **20A** (1989) 957.
11. A. S. ODDY and M. J. BIBBY, *Trans CSME* (1983) 25.
12. B. V. KUMAR, PhD thesis, IIT Kharagpur (1990).
13. M. JACOB, "Heat Transfer" (Wiley, 1956) p. 322.
14. H. S. CARSLAW and J. C. JAEGAR, "Conduction of Heat in Solids" (Oxford University Press, 1959) p. 266.
15. C. J. SMITHELLS, "Metals Reference Book", 5th Edn (Butterworths, 1976) p. 940.
16. E. KREYSZIG, "Advanced Engineering Mathematics" (Wiley Eastern, 1983) p. 848.
17. C. M. ADAMS, *Weld. J.* **37** (1955) 18-s.
18. S. V. PATANKER, "Numerical Heat Transfer and Fluid Flow" (McGraw-Hill, 1980) p. 57.
19. O. R. MYHR and O. GRONG, *Acta Metall. Mater.* **38** (1990) 449.
20. P. JHAVERI, W. G. MOFFATT and C. M. ADAMS, *Weld J.* **41** (1962) 12-s.
21. M. F. ASHBY and K. E. EASTERLING, *Acta Metall.* **32** (1984) 1935.
22. I. S. SOKOLINKOFF, "Advanced Calculus" (McGraw-Hill, 1939) p. 58.

Received 28 August 1990
and accepted 1 May 1991